

“Passive methods for airfoil noise reduction”

Seminarium Zakładu Aerodynamiki 13.01.2017r.

Autor: Witold Krusz

Promotor: Prof. hab. dr inż. Jacek Rokicki

Promotor pomocniczy: dr inż. Zbigniew Rarata

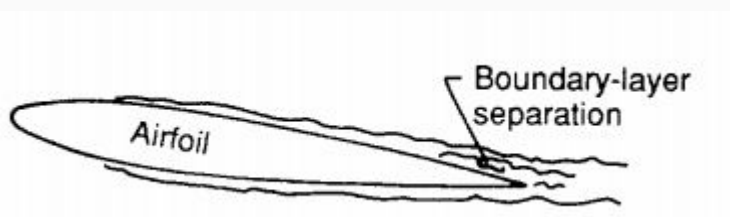
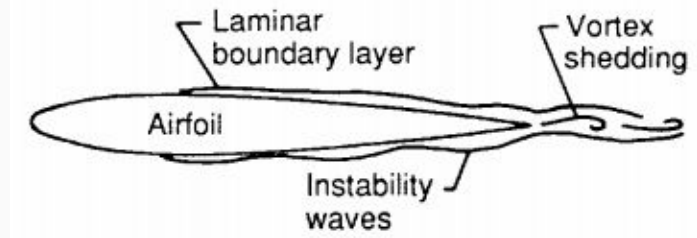
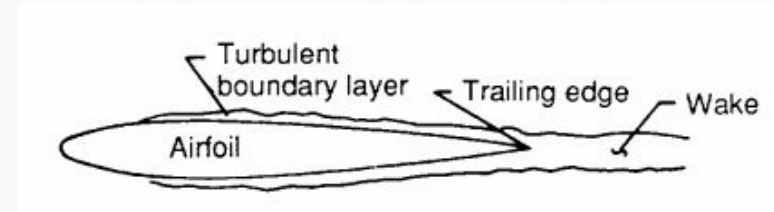
Characteristic of airfoil self noise

Airfoil self noise is due to the interaction between airfoil and turbulence produced in its own boundary layer and wake.

TBL- Turbulent boundary layer noise, noise is produced as turbulence passes over the trailing edge. Mainly broadband noise is generated.

LBL- Laminar boundary layer instability noise, Tonal noise emission, connected with broadband noise of wake.

BLS- For nonzero angles of attack, the flow can separate near the trailing edge on the suction side of the airfoil to produce trailing edge noise due to the shed turbulent vorticity.

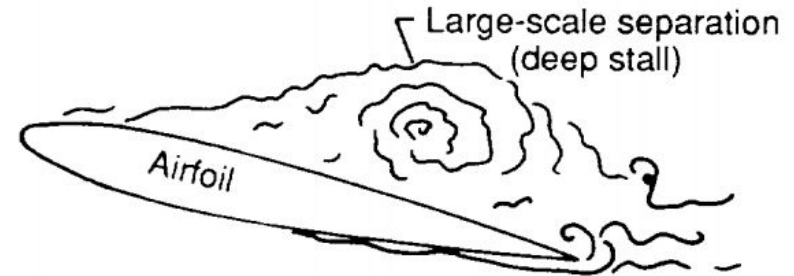


Airfoil self noise sources. Brooks et al.[1]

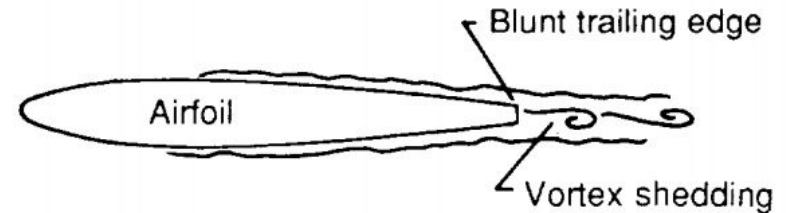
Characteristic of airfoil self noise

BLS- At very high angles of attack, the separated flow near the trailing edge gives way to large-scale separation (deep stall) causing the airfoil to radiate low-frequency noise similar to that of a bluff body in flow.

BN-Another type of airfoil noise is blunt noise, it is caused by vortex shedding occurring in the small separated flow region aft of a blunt. Typically, it increase level of broadband noise emission.



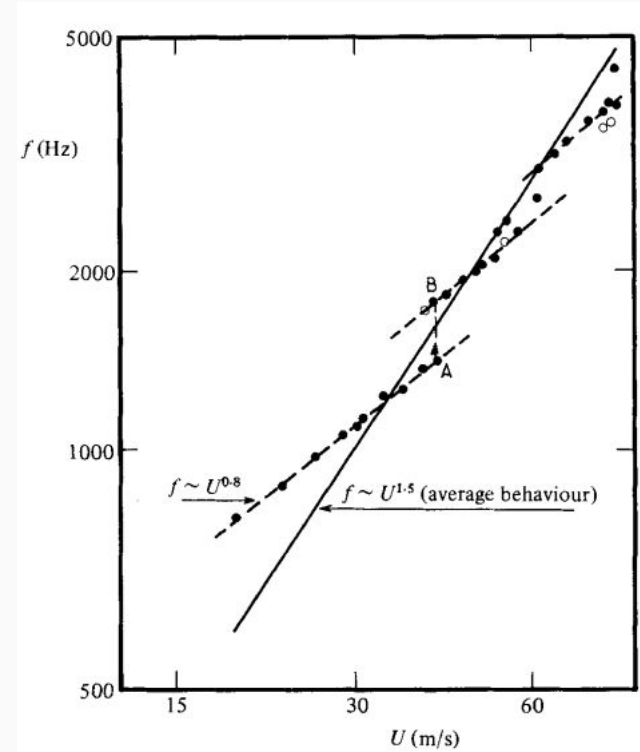
Separation-stall noise



Trailing-edge-bluntness—vortex-shedding noise

Airfoil boundary layer instability noise

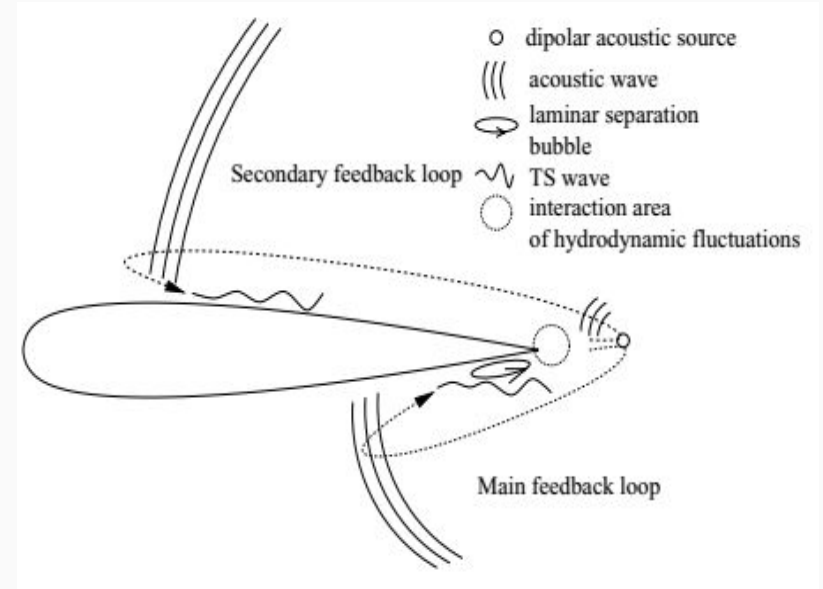
- Frequencies of the tonal components follow the $U^{0.8}$ relationship. (Tam[2])
- Generation of airfoil tonal noise is due to the feedback loop between the boundary layer on an airfoil pressure side and a dipole type acoustic source placed near the trailing edge.
- Separation bubble is a necessary condition for boundary layer instability noise. Separation bubble acts as an amplifier for the T-S waves.
- Desequesnes et al.[3] showed that instabilities on the suction side of an airfoil also play an important role in the generation of the tonal components. Therefore, it can be stated that the mechanism of airfoil instability noise generation consists of two feedback loops, i.e. the main loop on the airfoil pressure side and the secondary feedback loop on its suction side.



Peak frequencies vs flow velocity. Patterson et al.[2]

Airfoil boundary layer instability noise

- Frequencies of the tonal components follow the $U^{0.8}$ relationship. (Tam[2])
- Generation of airfoil tonal noise is due to the feedback loop between the boundary layer on an airfoil pressure side and a dipole type acoustic source placed near the trailing edge.
- Separation bubble is a necessary condition for boundary layer instability noise. Separation bubble acts as an amplifier for the T-S waves.
- Desequesnes et al.[3] showed that instabilities on the suction side of an airfoil also play an important role in the generation of the tonal components. Therefore, it can be stated that the mechanism of airfoil instability noise generation consists of two feedback loops, i.e. the main loop on the airfoil pressure side and the secondary feedback loop on its suction side.



Mechanism of boundary layer instability noise generation. Desequesnes et al.[3]

DNS MODEL:

- Number of cell: 60 mln
- $Y^+=0.6$ on first cell-layer
- Density based solver
- Second order upwind spatial discretization scheme
- Unsteady second order implicit formulation

In order to obtain the 3D flow simulations, standard periodic boundary conditions were imposed on both sides of the computational domain.

Reynolds Number: 200 000

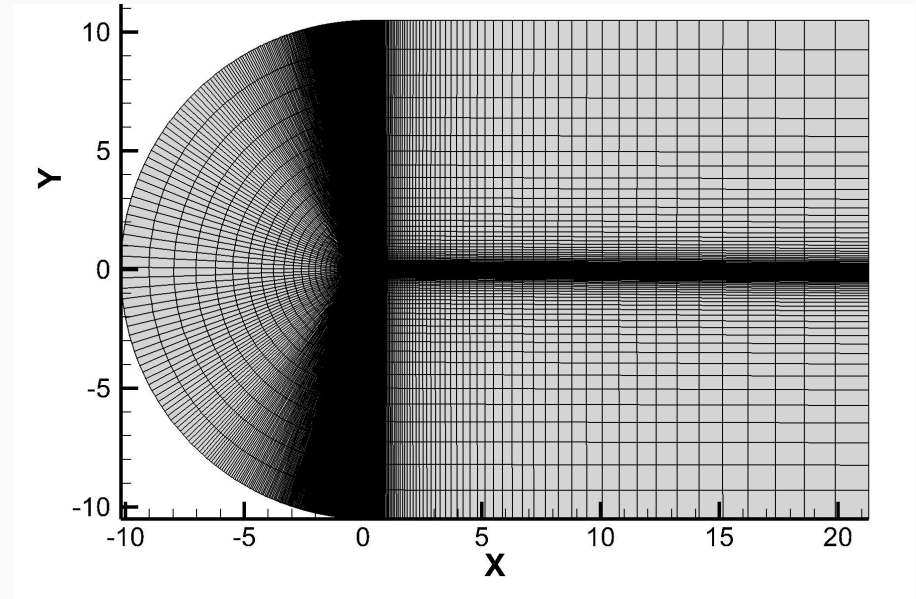
Mach Number: 0.03

Airfoil chord: 0.3 m

Inflow velocity: 10m/s

Angle of attack: 2 degrees

Spanwise dimension of computational domain: 0.036m



Computational domain. C-mesh type

LES MODEL:

- Number of cell: 50 mln/70 mln (serrated models)
- $Y^+ = 0.8 \sim 0.9$ on first cell-layer
- Density based solver
- Second order upwind spatial discretization scheme
- Unsteady second order implicit formulation
- Smagorinsky-Lilly subgrid-scale model with dynamic stress was applied

In order to obtain the 3D flow simulations, standard periodic boundary conditions were imposed on both sides of the computational domain.

Reynolds Number: 200 000

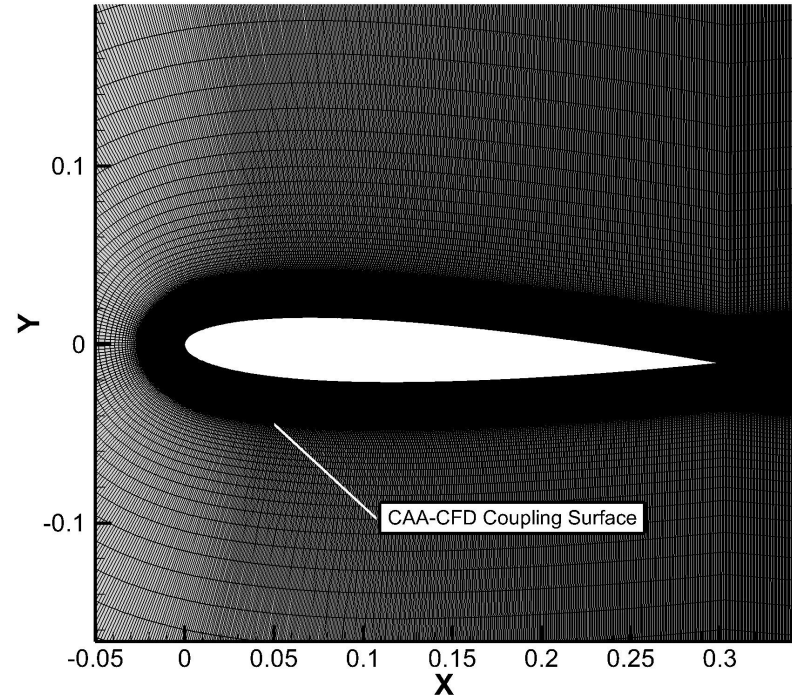
Mach Number: 0.03

Airfoil chord: 0.3 m

Inflow velocity: 10m/s

Angle of attack: 2 degrees

Spanwise dimension of computational domain: 0.036m,
0.045 m for serrated cases



Computational domain. Near airfoil region and CAA-CFD Coupling Surface

Acoustic Power and Intensity

For source free region, total energy is conserved:

$$\frac{\partial E}{\partial t} + \nabla \cdot \mathbf{I} = 0.$$

Acoustic Intensity and Acoustic Energy density for homentropic and irrotational mean flows can be defined:

$$\mathbf{I} = \left(\frac{p'}{\rho_0} + \mathbf{u}' \cdot \mathbf{u}_0 \right) \left(\rho_0 \mathbf{u}' + \frac{p'}{c_0^2} \mathbf{u}_0 \right), \quad E = \frac{p'^2}{2\rho_0 c_0^2} + \frac{\rho_0 \mathbf{u}'^2}{2} + \rho' (\mathbf{u}' \cdot \mathbf{u}_0).$$

For steady and periodic flows, with no acoustic sources the average of energy implies that:

$$\nabla \cdot \bar{\mathbf{I}} = 0,$$

Time averaged acoustic intensity is given by:

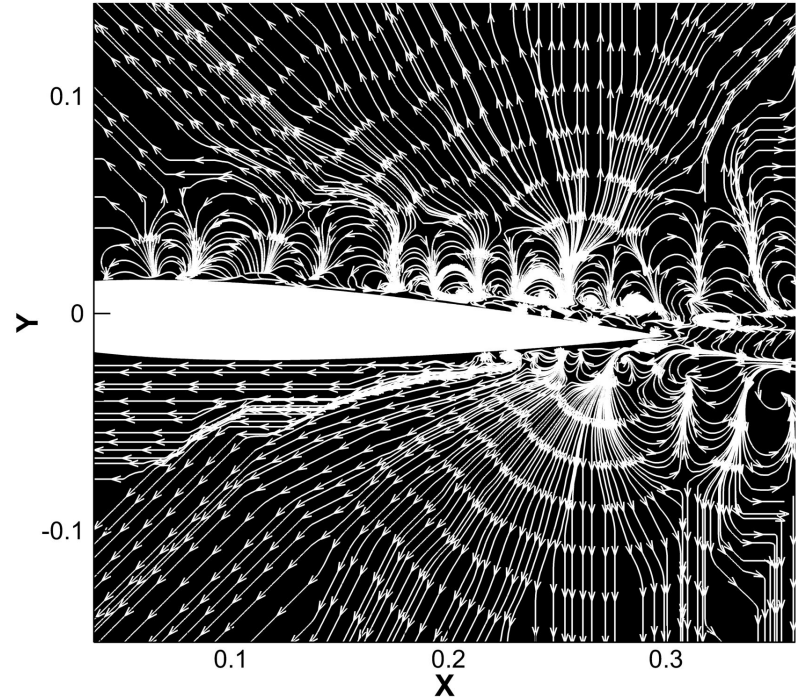
$$\bar{\mathbf{I}}(\mathbf{x}) = \frac{1}{T} \int_T \mathbf{I}(\mathbf{x}, t) dt.$$

Acoustic power crossing surface S:

$$P = \int_S \bar{\mathbf{I}} \cdot \mathbf{n} dS$$

Acoustic intensity in the frequency domain for homentropic and irrotational flow::

$$\bar{\mathbf{I}}(\mathbf{x}) = \frac{1}{2} \left[\text{Re}\{\tilde{p}\tilde{\mathbf{u}}^*\} + \rho_0 \text{Re}\{(\mathbf{u}_0 \cdot \tilde{\mathbf{u}})\tilde{\mathbf{u}}^*\} + \frac{1}{c_0^2} \mathbf{u}_0 (\mathbf{u}_0 \cdot \text{Re}\{\tilde{p}\tilde{\mathbf{u}}^*\}) + \frac{1}{c_0^2 \rho_0} \mathbf{u}_0 |\tilde{p}|^2 \right].$$

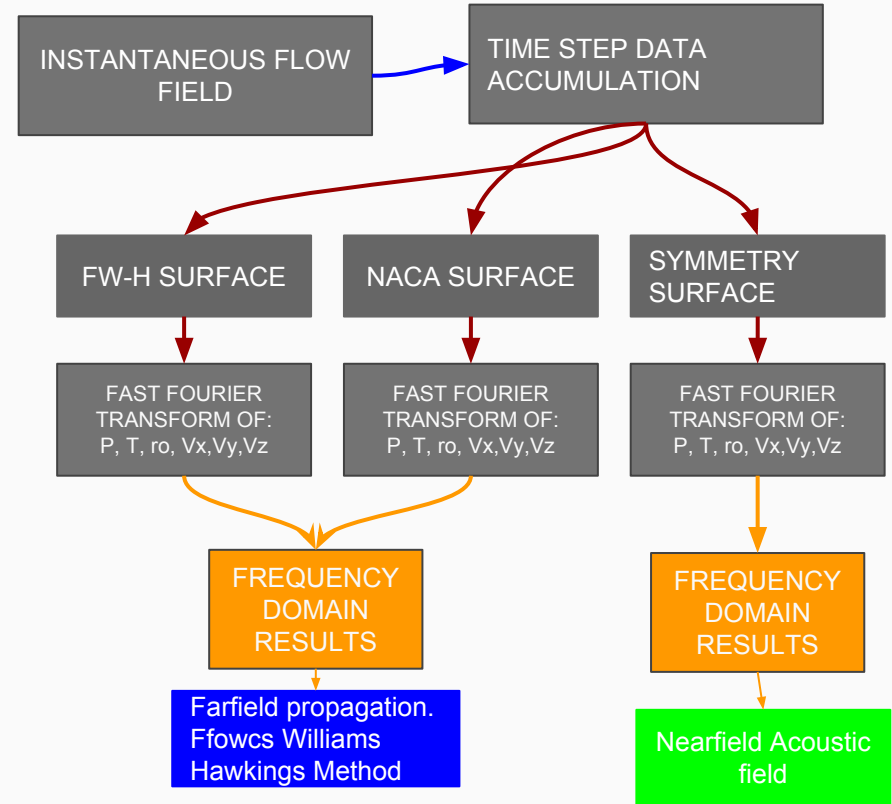
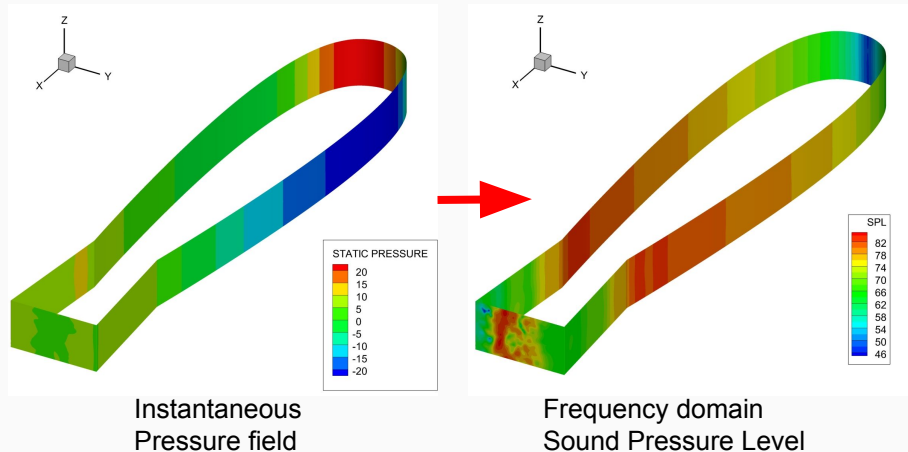


Acoustic Intensity streamlines for DNS case.

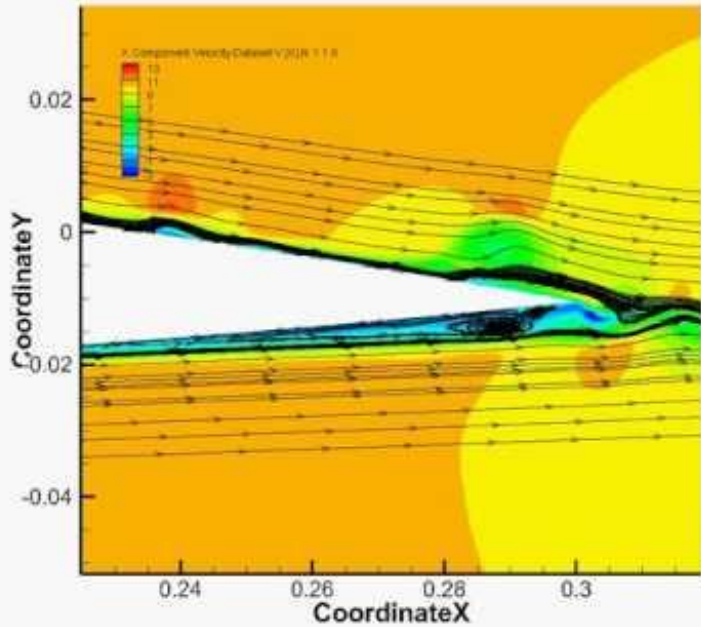
CAA-CFD Coupling

CFD data coupling with farfield propagation is realized in the following way:

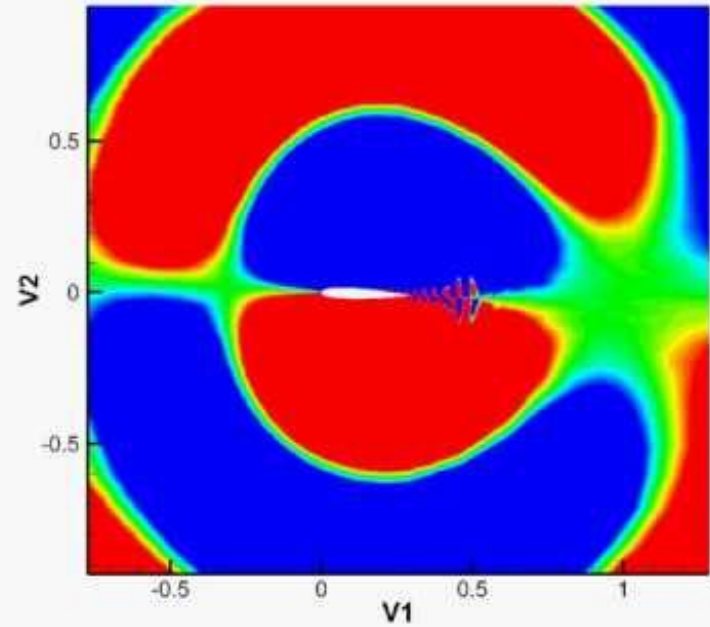
- Field data is exported every hundredth time steps to allow analysis frequency range between 0 and 1250 Hz
- Accumulated data transformation using Fast Fourier transform.
 - Hamming windowing function of signal
 - Fourier transformation of p', T', ρ', V'



CAA-CFD Coupling



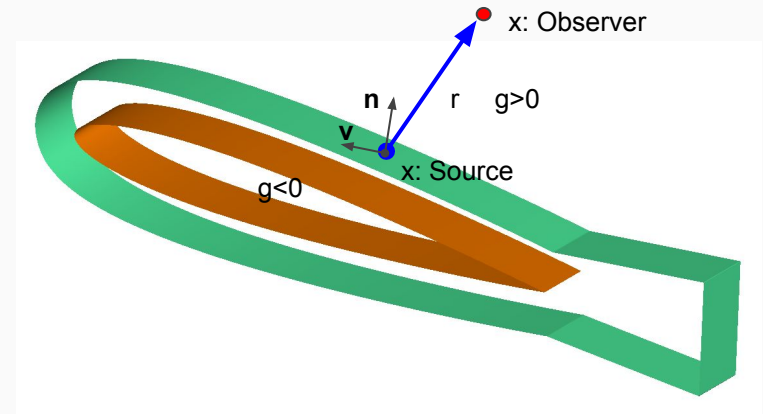
Instantaneous velocity field, flow around NACA 0012 airfoil. Direct Numerical Simulation.



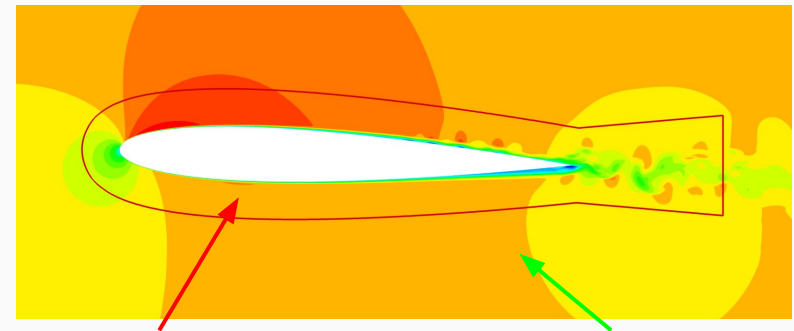
Frequency domain flow around NACA 0012 airfoil. Real Part of Acoustic Pressure for 260 Hz frequency.

Far-field Propagation

- The Ffowcs-Williams and Hawkings method were used for the far-field reconstruction.
- Input data for FWH method is collected from the **FWH surface**.
- FWH surface is defined on offset surface to the airfoil geometry (25mm above airfoil surface), with extended region of 100mm behind the trailing edge
- CFD domain:
 - Generation of acoustic sources (boundary layer/wake)
 - Direct acoustic propagation by Navier-Stokes equation
- Outer region: Acoustic waves damping before boundary conditions. (Buffer zone using stretched elements)



CAA model for far-field propagation

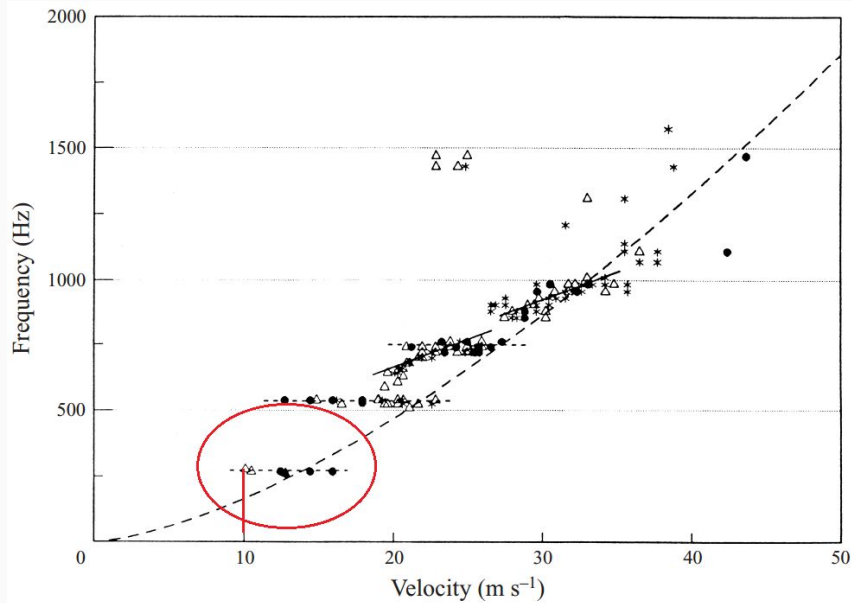


CFD (DNS/LES) acoustic sources

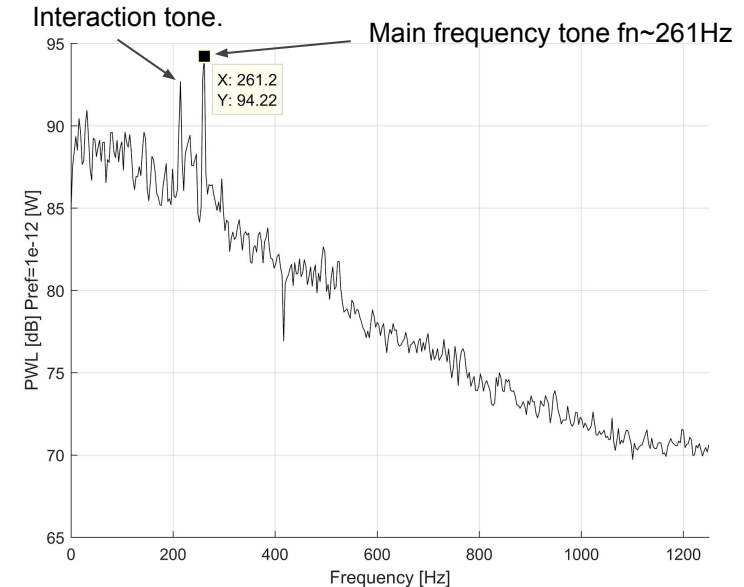
Outer region of acoustic waves damping

Validation of DNS results.

- Basing on experimental results (Lowson et al. [4]), main tonal frequency should be equal to 260 [Hz].
- Acoustic Power spectrum presents well correlation of main tonal frequency $f_n \sim 261$ Hz obtained from Direct Numerical Simulation with Lowson et al experimental data.



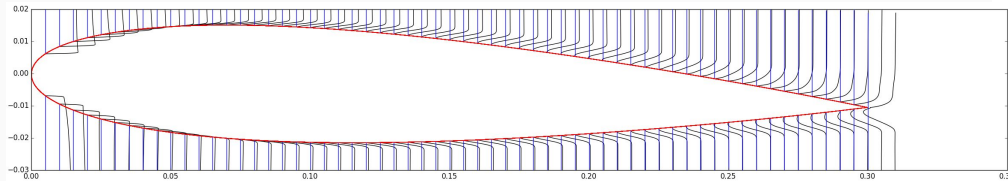
Peak frequencies vs flow velocity. Lowson et al.[4] experimental data.



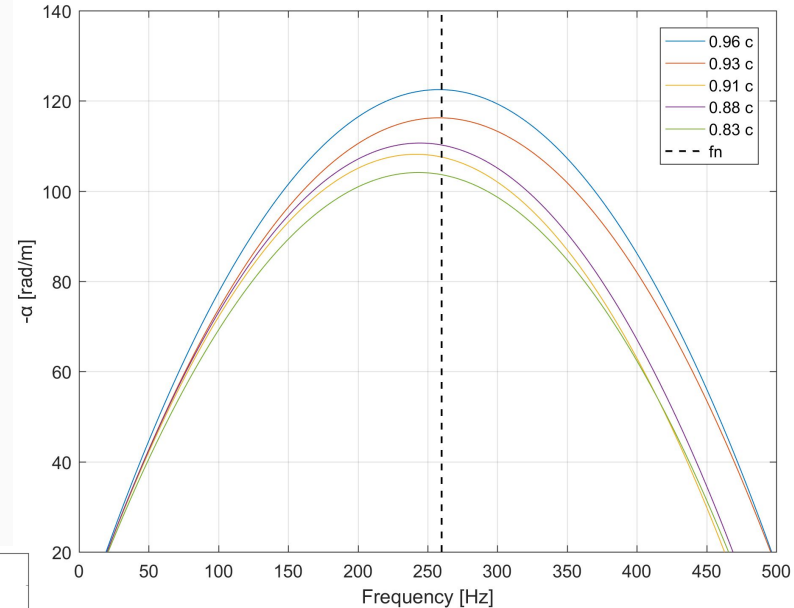
Acoustic Power spectrum from Direct Numerical Simulation, Computed at FWH surface. Very good comparison with experimental data

Validation of DNS results:

- Spatial stability analysis of boundary layer velocity profiles near trailing edge shows that most amplified growth rates are well correlated with main boundary layer instability tone.
- Solution for Spatial Modes of Orr-Sommerfeld Equation based on Chebyshev Matrix Method. Danabasoglu et al.[8]
 - Quasi parallel flow (Limitation to 2D cases)
 - Velocity profile from Direct Numerical Simulation, with “equally spaced interpolation”



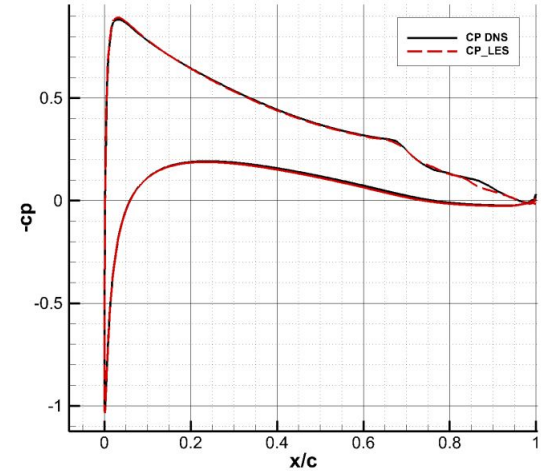
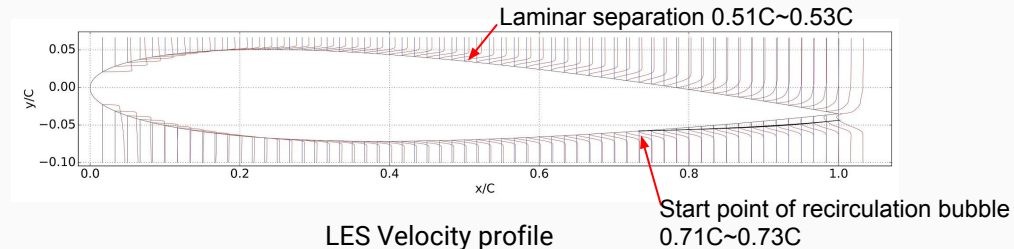
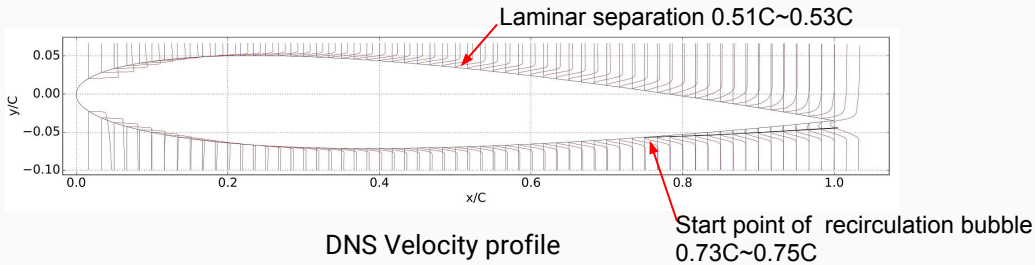
Boundary layer velocity profiles from DNS simulation.



Spatial stability analysis results.

Comparison of DNS and LES models:

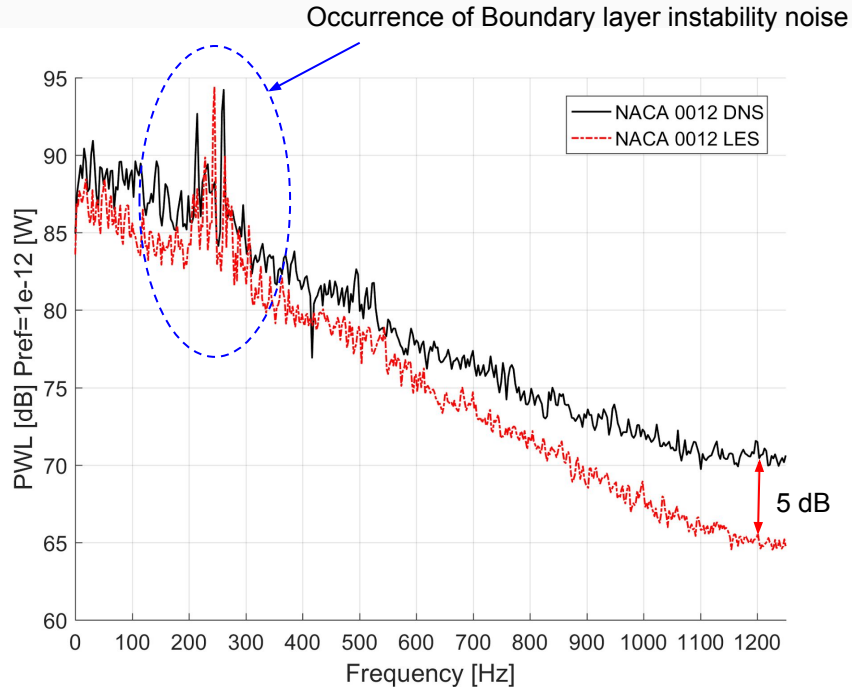
- Some differences on time averaged velocity field in localization of the laminar separation bubble.
- LES solution slightly over predicts the pressure coefficient at the leading edge on the suction side.
- C_p distribution predicted by the LES simulation is more irregular close to the trailing edge



	Exp.	DNS	LES
C_d	0.012	0.012	0.013
C_l	0.309	0.316	0.307

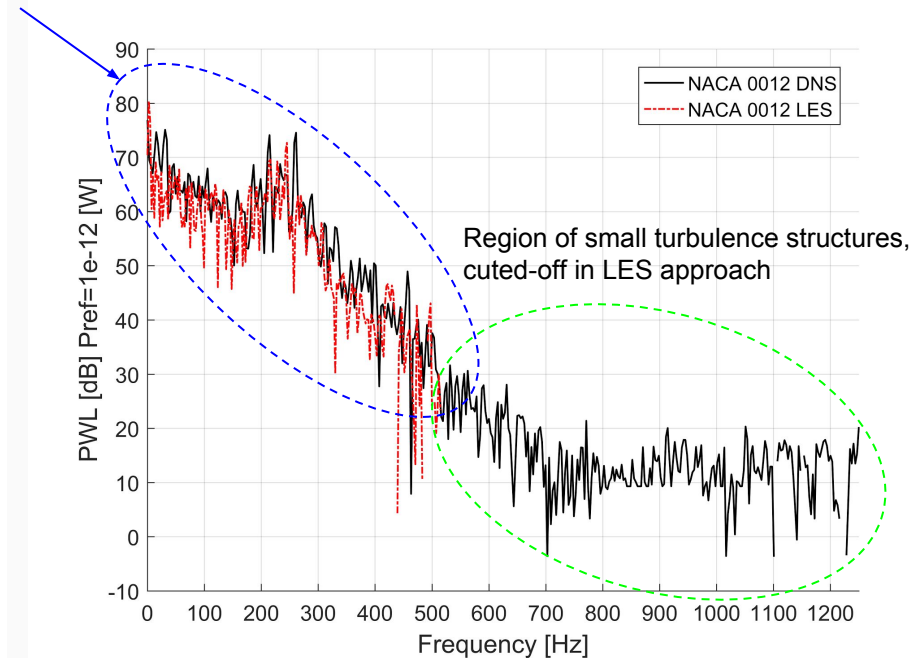
DNS agree well with experimentally determined values. There is, however, some discrepancy of approximately 2% in the lift coefficient. The LES gives also good match to the experimental data, although the drag coefficient is over predicted by 8%.

Comparison of the PWL at the FWH surface. Between DNS and LES:



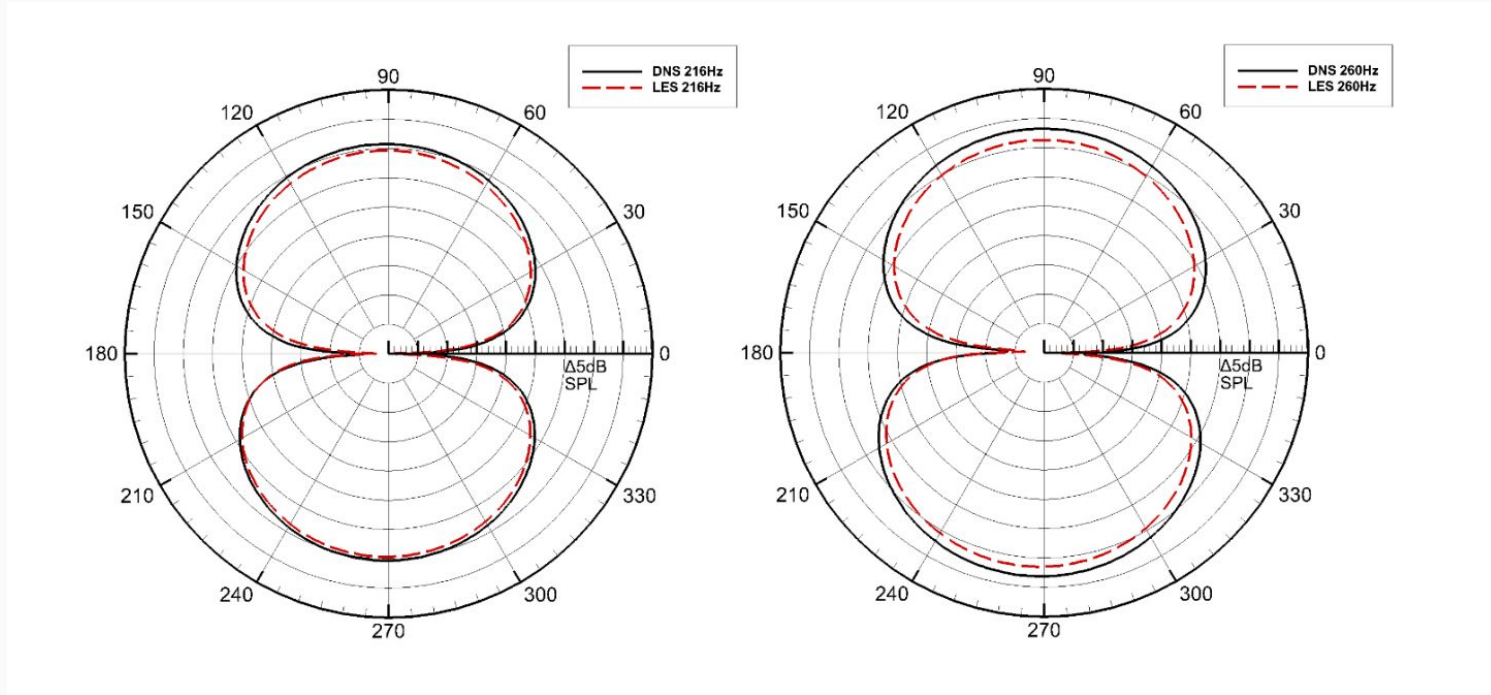
Comparison of power spectrums. Computed on closed FWH surface.

- 5dB difference in broadband noise prediction.
- Well comparison of tonal noise region.



Comparison of power spectrums. Computed on opened FWH surface.

Comparison of SPL in far-field between DNS and LES:

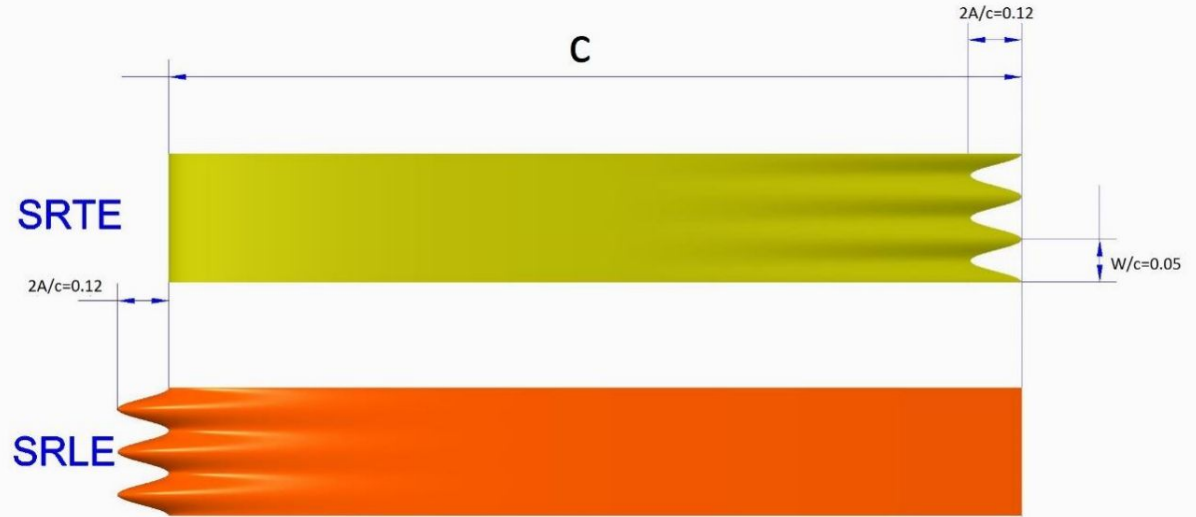


Comparison of the far-field (20c) directivity of the SPL between DNS and LES simulations for the NACA 0012 airfoil in clean configuration. Left hand side plot shows the directivity for 216Hz, whereas right hand side for 260Hz.

- Very good comparison of SPL in far-field between LES and DNS for main tonal components.
- Almost ideal dipolar sound emission from trailing edge.

Investigation of leading and trailing edge serrations:

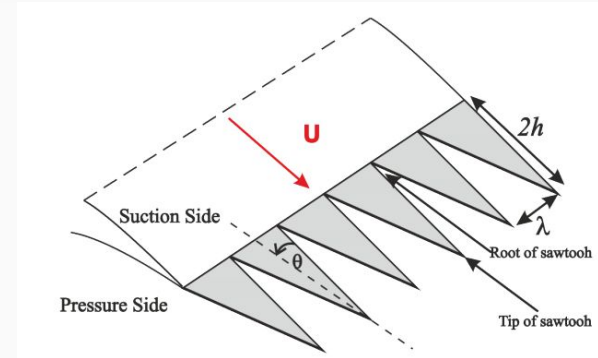
- Geometric configuration of trailing edge serrations based on M.S Howe [5] and L.E Jones et al.[6] works.
- Similar geometrical parameters of serration were used for leading edge serration model.
- The geometrical details of serration according to chord is: $W/c=0.05$ and the height of serration teeth is $A/c=0.12$.



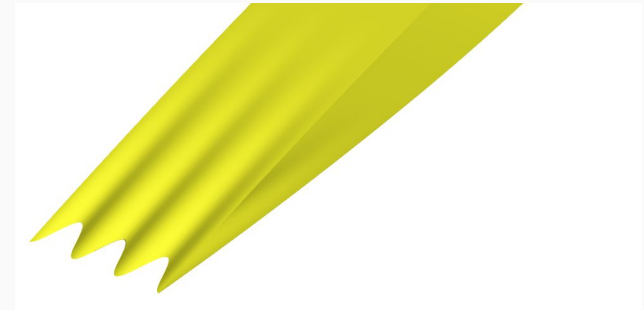
Serrated trailing edge (SRTE) and serrated leading edge (SRLE) geometry definition.

Investigation of leading and trailing edge serrations:

- Large Eddy Simulation approach. (Reduction of computational time)
- Comparison of aerodynamic performances:
 - Leading Edge Serration:
 - Reduction of lift coefficient up to 37%
 - Increase of drag coefficient up to 4.5%
 - Trailing Edge Serration:
 - Reduction of lift coefficient up to 10%
 - Increase of drag coefficient up to 7.5%
- Serrated trailing edge geometry is well examined in turbulence interaction cases. This approach gives significant reduction of broadband noise.
- Typical Serrated trailing edge geometry ensure broadband noise reduction by modification of acoustic waves scattering on trailing edge and braking of turbulent structures.

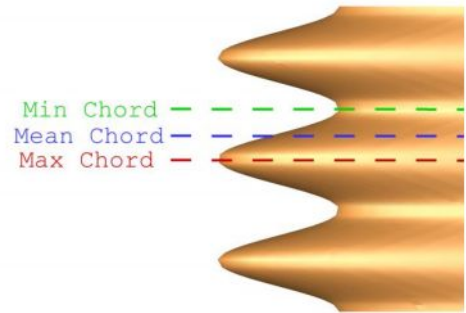
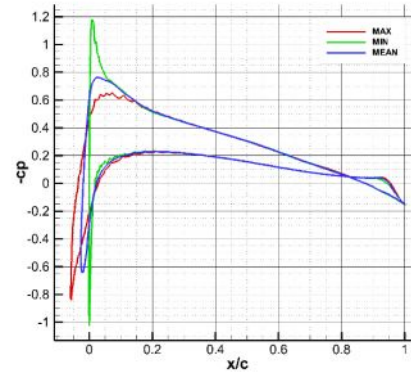
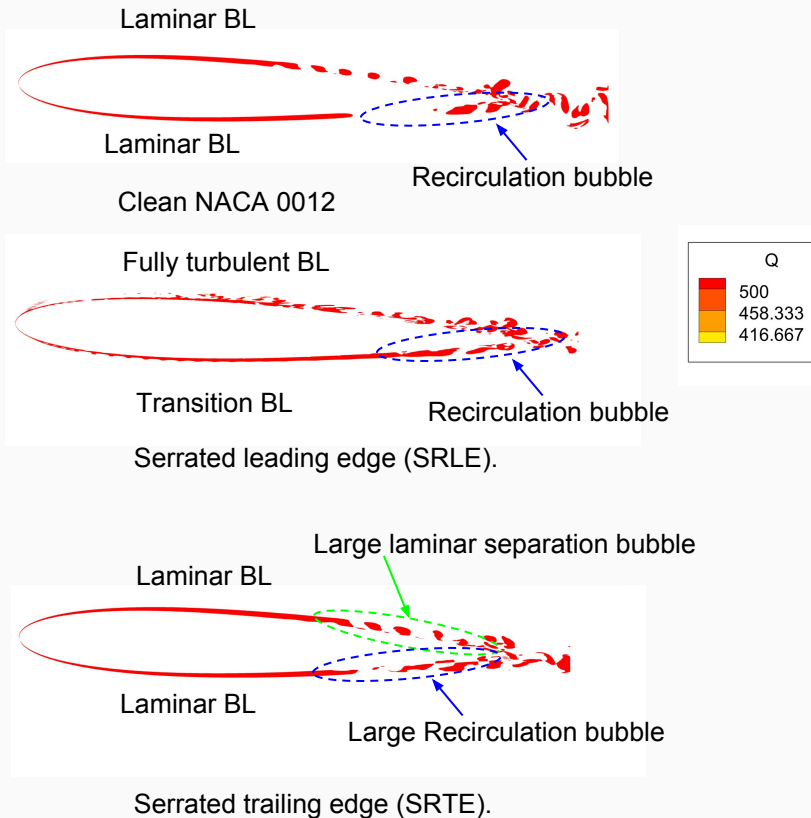


Typical Serrated trailing with insert plate. Gruber et al.[7]

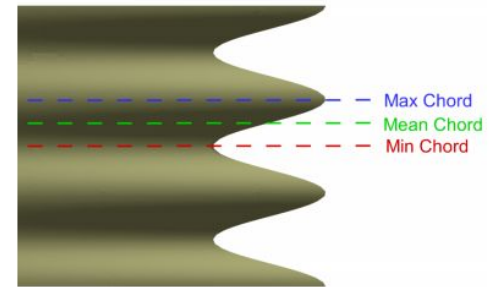
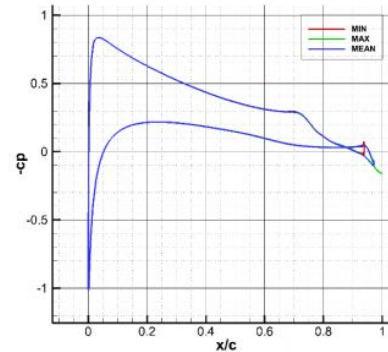


3D SRLE airfoil from current studies.

Investigation of leading and trailing edge serrations:

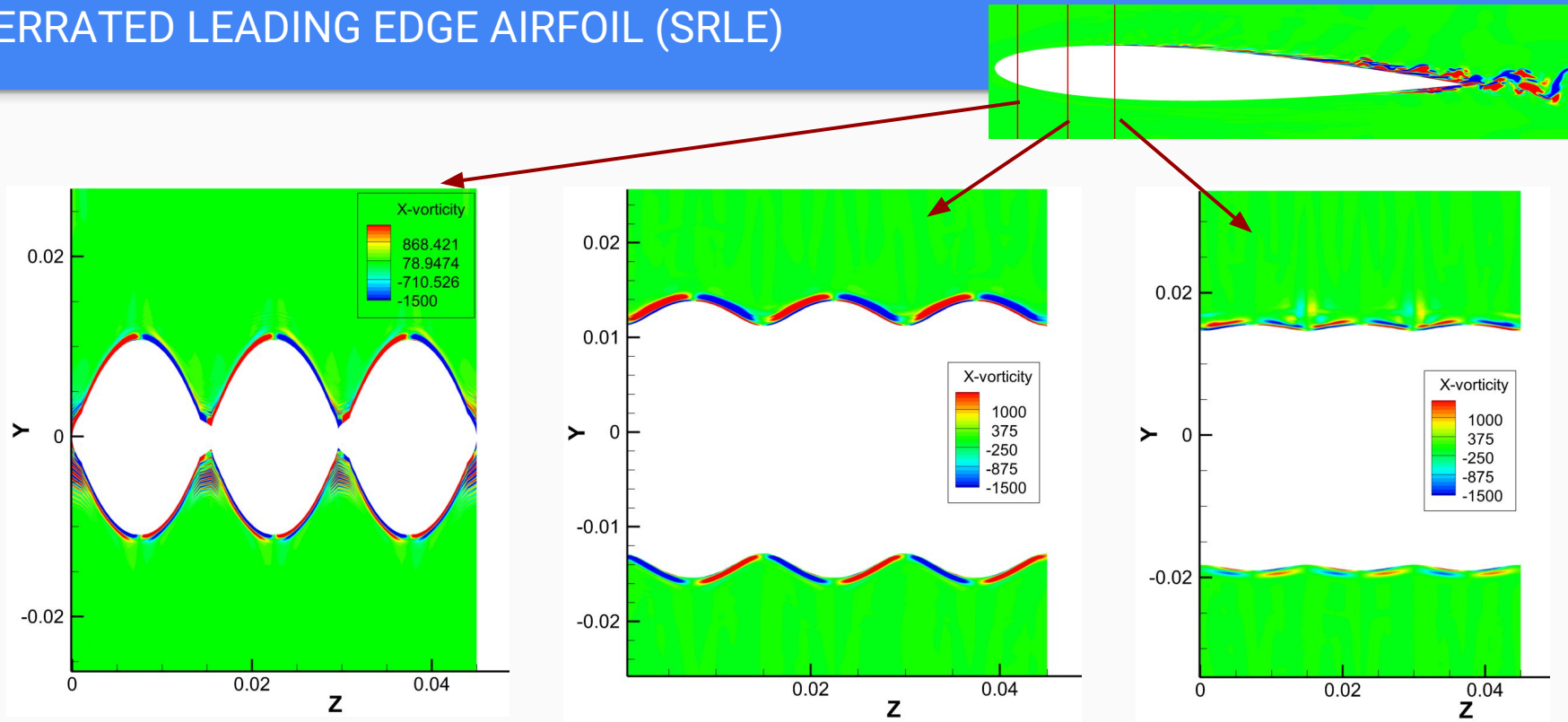


Pressure Coefficient of SRLE airfoil, with plot localization.



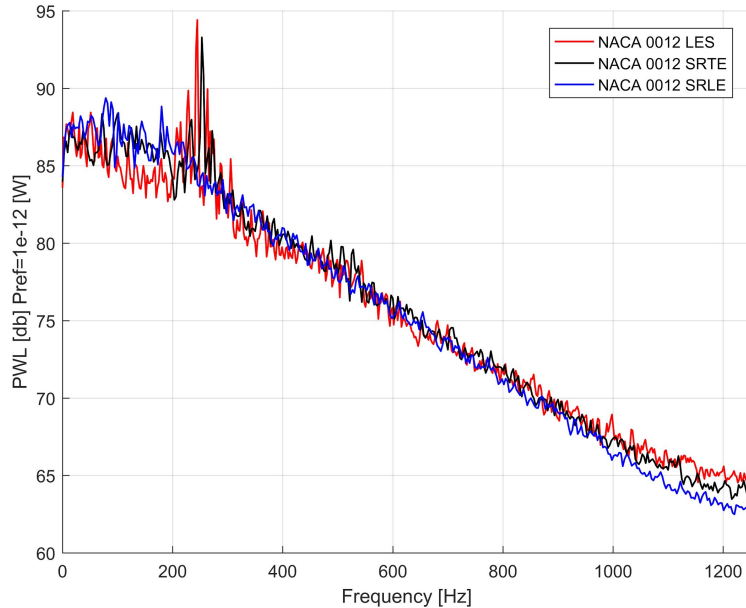
Pressure Coefficient of SRTE airfoil, with plot localization.

SERRATED LEADING EDGE AIRFOIL (SRLE)



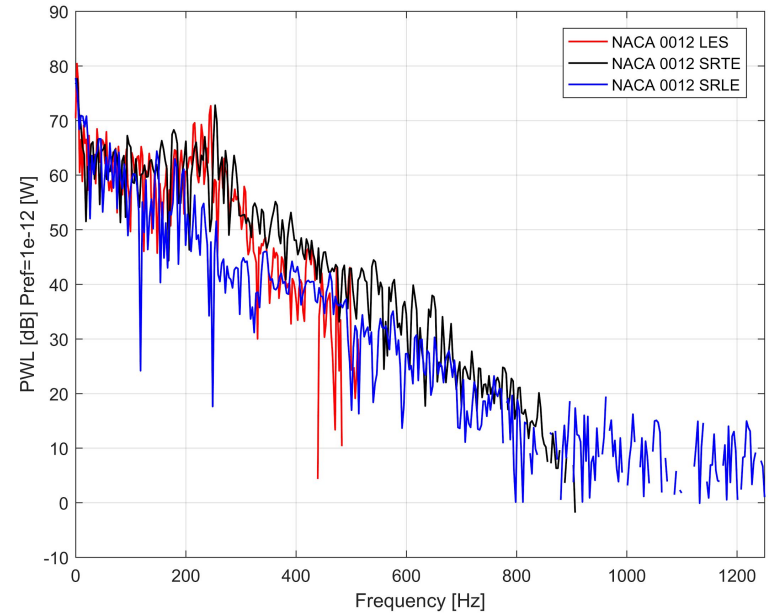
The noise reduction mechanism in Serrated Leading edge model is attributed to the chordwise vortices induced by the leading-edge serrations which can affect airfoil downstream boundary layer flow and may trigger bypass transition which can suppress T-S wave and cut-off boundary layer instability noise. This kind of forced boundary layer transition directly from leading edge show significant noise reduction in turbulent interaction cases and also in boundary layer instability noise regime.

Comparison of PWL at the FWH surface for CLEAN LES, SRTE, SRLE cases:



Comparison of power spectrums. Computed on closed FWH surface.

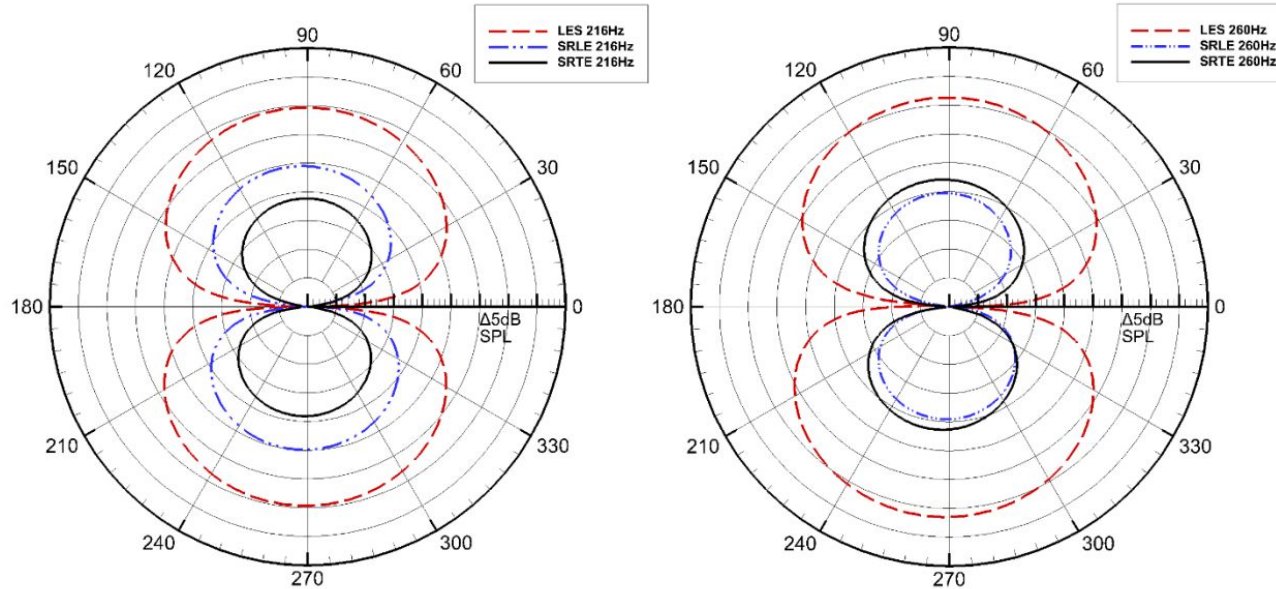
- SRLE: Attenuation of tones amplitude and frequency reduction (245->180)
- SRTE: Increase of main tone frequency, minimal amplitude reduction.



Comparison of power spectrums. Computed on opened FWH surface.

- SRLE: Significant reduction on tonal and broadband noise. Wider spectrum of broadband noise, mainly caused by full turbulence BL on suction side.
- SRTE: Frequency offset between clean LES case and SRTE frequency. Broadband and tonal noise reduction mainly by modification of acoustic waves scattering on trailing edge

Comparison of far-field acoustic propagation:



The comparison of the far-field (20c) directivity of the SPL between the NACA0012 airfoil in clean configuration and the NACA0012 airfoil with the leading edge and trailing edge serration. Left hand side plot shows the directivity for 216Hz, whereas right hand side for 260Hz.

- For both serrated cases we can observe significant reduction of SPL in far-field.
- Similar as in Clean geometry configuration we en observe almost ideal dipolar sound emission.
- For lower frequency we can observe better SPL reduction for SRTE model, for higher frequency SRLE model had better efficiency.

Conclusions:

- Validation of Large Eddy Simulation against Direct Numerical simulation and experimental data have proven that the Large Eddy Simulation effective tool for modeling boundary layer instability noise.
- Leading edge serration:
 - Good performance in reduction of tonal components, reduction of frequency and amplitude
 - Worsening of aerodynamic performances
- Trailing edge serration:
 - Reduction of tonal components mainly by different acoustic waves mechanism of trailing edge. Reduction of tonal component visible only on full spectrum with wake.
 - Worsening of aerodynamic performances.
 - Analysis of classical solution with insert plate could be useful to verify this approach.
- Elaboration of new geometries/approaches for boundary layer noise reduction maintaining the aerodynamic performance is needed.

References:

1. T. F. *Brooks*, D. S. Pope, M. A. Marcolini, "*Airfoil Self-Noise and Prediction*" NASA. Reference. Publication. 1218. July. 1989.
2. Paterson, R. W, Vogt, P. G, Fink, M. R, Munch, C. L, "Vortex noise of isolated airfoils", *Journal of Aircraft*, Vol. 10, No. 5, 1973, pp. 296-302.
3. Desquesnes, G, Terracol, M, Sagut P, "Numerical investigation of the tone noise mechanism over laminar airfoils", *J. Fluid Mech*, Vol. 591 2007, pp. 155-182.
4. Lawson, M. V, Fiddes, S. P, Nash, E. C, "Laminar boundary layer aeroacoustic instabilities", 32nd Aerospace Sciences Meeting & Exhibit, Reno, 1994.
5. Howe, M. S, "Noise produced by sawtooth trailing edge", *J. Acoust. Soc. Am*, Vol. 90, 1991, pp 482-487.
6. Jones, L. E, Sandberg R. D, "Acoustic and hydrodynamic analysis of the flow around an aerofoil with trailing-edge serrations", *J. Fluid Mech*, Vol. 706 2012, pp. 295-322.
7. M. Gruber, P. F. Joseph, "On the mechanism of serrated airfoil trailing edge noise reduction" 17th AIAA/CEAS Aeroacoustics Conference (32nd AIAA Aeroacoustics Conference) 05 - 08 June 2011, Portland, Oregon
8. G. Danabasoglu, S. Bringen, "A Chebyshev matrix method for spatial modes of the Orr-Sommerfeld equation" NASA-CR-4247, NAS 1.26:4247

The authors would like to acknowledge the Interdisciplinary Centre for Mathematical and Computational Modelling (ICM) at the University of Warsaw for allowing to use the high power computing facilities under a grant No. GA65-18